



ELSEVIER

Contents lists available at ScienceDirect

Materials Letters

journal homepage: www.elsevier.com/locate/matlet

Thermal transport in graphene fiber fabricated by wet-spinning method



Huan Lin^a, Hua Dong^{a,*}, Shen Xu^b, Xinwei Wang^{a,b}, Jingkui Zhang^a, Yongchun Wang^a

^a School of Environmental and Municipal Engineering, Qingdao University of Technology, Qingdao, Shandong, 266033 PR China

^b Department of Mechanical Engineering, Iowa State University, 2010 Black Engineering Building, Ames, IA, 50011 USA

ARTICLE INFO

Article history:

Received 1 June 2016

Received in revised form

16 July 2016

Accepted 19 July 2016

Available online 20 July 2016

Keywords:

Carbon materials

Thermal properties

Graphene fiber

Graphene oxide

Defects

ABSTRACT

Graphene-based materials are usually expected to be good thermal conductors. Here, we report on the low thermal diffusivity of free-standing graphene fibers (GFs) fabricated by wet-spinning method. The GF sample mainly consists of freestanding graphene oxide. The radiation effect is excluded by measuring GFs of different lengths. The thermal diffusivity of the suspended GF sample is determined at $(2.0\text{--}2.08) \times 10^{-6} \text{ m}^2 \text{ s}^{-1}$, and the corresponding intrinsic thermal conductivity is 1.14–1.18 W/m K. The low thermal conductivity is mainly attributed to the large thermal contact resistance and very strong phonon scattering at grain boundaries. The finding will be beneficial for thermal design of GF-based thermal energy applications.

© 2016 Elsevier B.V. All rights reserved.

1. Introduction

Graphene, a flat monolayer of carbon atoms tightly packed into a two-dimensional (2D) honeycomb lattice, is the basic building block for carbon materials of all other dimensionalities [1]. It attracted intensive research attention in recent years because of its fascinating properties [2,3], especially for its extremely high intrinsic thermal conductivity of suspended single-layer graphene ($> 2000 \text{ W/m K}$). [4–8].

The strong, conductive and flexible GFs have the promise in applications such as functional textiles and supercapacitors devices [9]. The neat GFs were first fabricated from concentrated Graphene oxide (GO) liquid crystal in 2011 using wet-spinning methodology by Xu [10]. Cheng developed a one-step dimension-confined hydrothermal strategy to fabricate neat GFs from aqueous GO suspensions [9]. Compared with the extensive research about thermal transport in graphene, little attention has been paid to GF. Rouhollah [11] measured the thermal conductivity of the GO fiber is 1435 W/m K^{-1} at room temperature. Tian [12] measured thermal properties of the regenerated cellulose/graphene composite fibers.

In this work, the thermal diffusivity of GF samples is measured using the transient electro-thermal (TET) technique. By measuring GFs of different lengths, we can exclude the radiation effect and obtain the intrinsic thermal diffusivity.

2. Materials and methods

The GF samples used in this work were purchased from JCNANO Company. Relevant chemical preparation details can be referenced in literature [13]. Cross-linked network structure and wrinkled surface of GF can be clearly observed in Fig. 1a–c. The energy dispersive spectroscopy (EDS) result shows that the primary compositions are carbon (68.45 wt%), oxygen (23.17 wt%), calcium (3.24 wt%) and sulfur (2.43 wt%). It indicates that GO is still the main component in our GF sample and it has only been partially reduced.

The GF sample is also characterized using Raman spectroscopy. In Fig. 1d, this GF clearly shows two major peaks, 1583 cm^{-1} (G band) and 1340 cm^{-1} (D band). There is no peak at 2700 cm^{-1} in Fig. 1d. It means that the GF contains few graphene structures. Combined with the EDS and SEM results, we conclude that there are strong structural defects in our GF sample and such continuous fiber mainly consists of free-standing GO.

The TET technique is employed to measure the thermal diffusivity of the GF samples of different lengths [14]. The schematic diagram of TET experiment setup is shown in Fig. 2a. During the whole measurement, Joule heat is induced by feeding a step current over a GF sample. The sample will experience a quick temperature rise to the thermally steady state. As graphene is a kind of semiconductor, the temperature rise of the sample will cause a drop in electrical resistance and thus lead to an overall voltage decrease.

* Corresponding author.

E-mail address: dhua1959@hotmail.com (H. Dong).

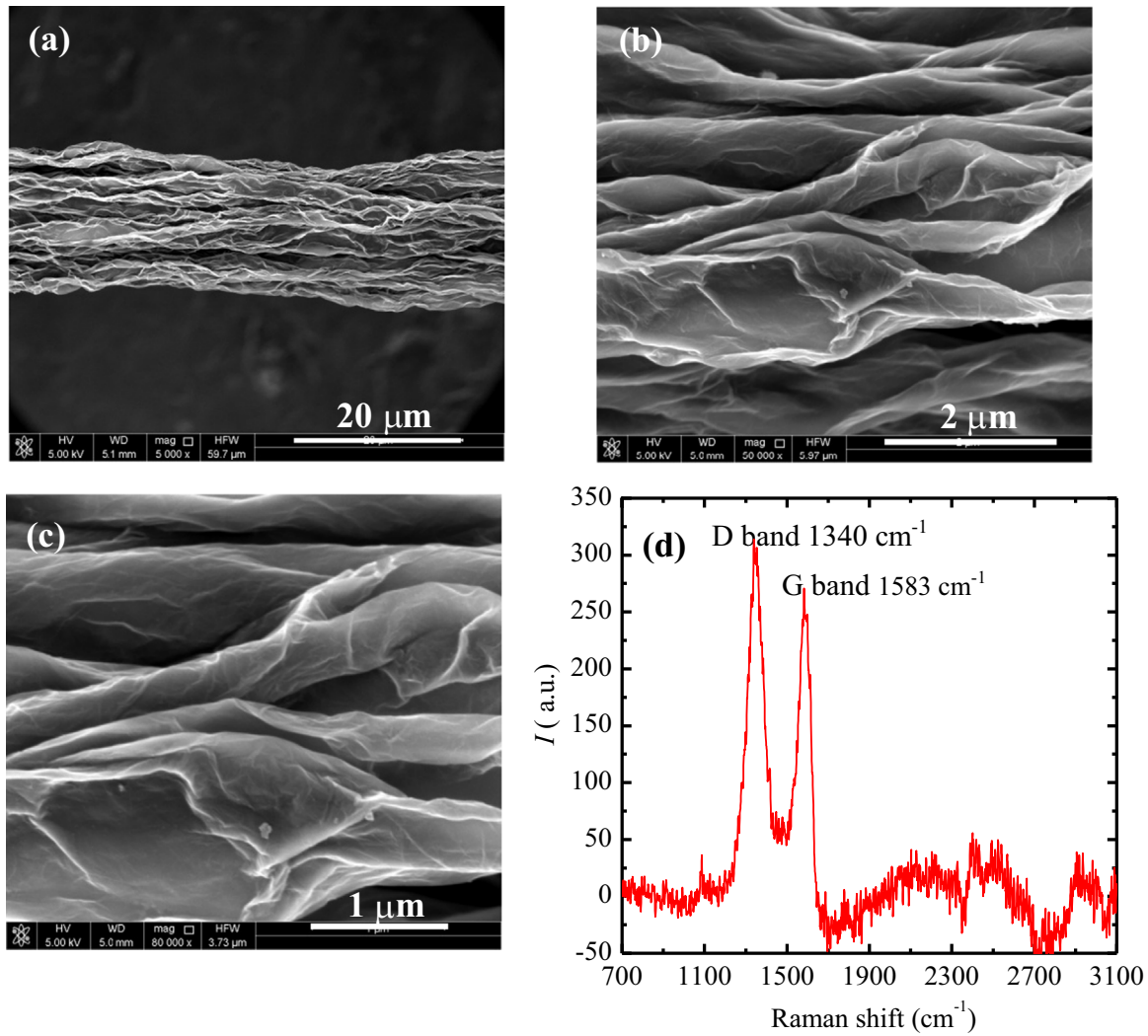


Fig. 1. SEM and Raman spectra images of GF studied in this work. (a), (b), and (c): SEM images of GF from low to high resolutions. (d): Raman spectrum of the GF sample.

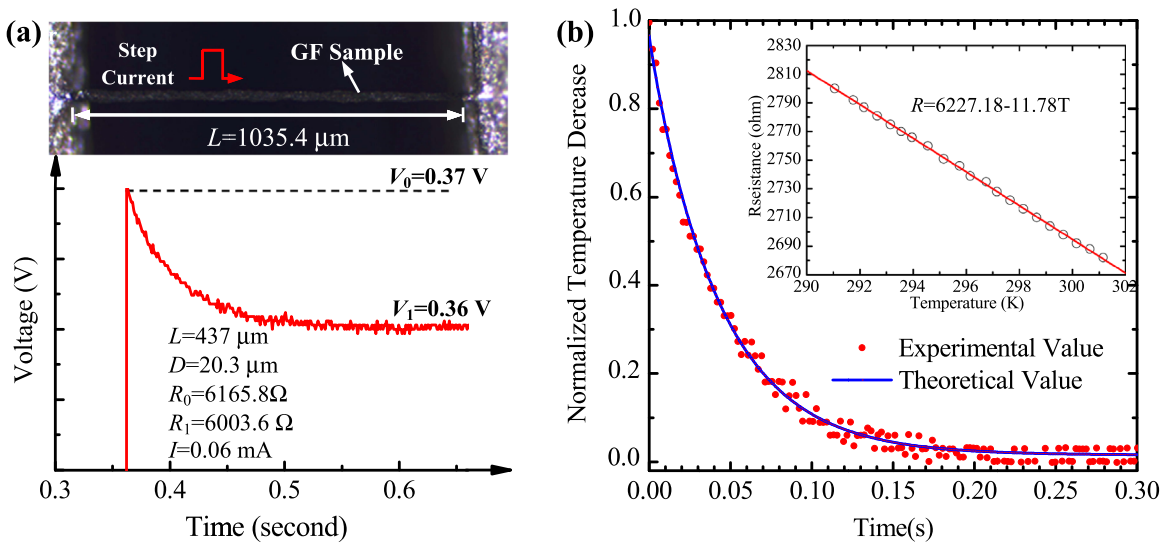


Fig. 2. (a). Experimental data for one GF (sample 1-1). (b). Comparison between theoretical fitting and experimental data for the normalized temperature rise versus time (sample 1-1). The inset shows the linear fitting for the resistance change against temperature for one general GF sample (416.3 μm long and 17 μm in diameter).

The heat transfer governing equation for the sample can be expressed as [15]:

$$\frac{1}{\alpha} \frac{\partial \theta(x, t)}{\partial t} = \frac{\partial^2 \theta(x, t)}{\partial x^2} + \frac{I^2 R_0}{k L A_c} + \frac{1}{k} \frac{16 \epsilon_r \sigma T_0^3}{D} \theta, \quad (1)$$

where α is thermal diffusivity, and k is thermal conductivity. A_c is the cross-sectional area and equals to $\pi D^2/4$. I is the current fed through the sample and R_0 is the resistance of the sample before heating. After careful numerical and mathematic deduction, we can get:

$$\alpha_{\text{measure}} = \alpha + \frac{1}{\rho c_p} \frac{16 \epsilon_r \sigma T_{\text{ave}}^3}{D} \frac{L^2}{\pi^2}, \quad (2)$$

where ρc_p is volumetric specific heat, T_{ave} is the average temperature. From this equation, the measured thermal diffusivity of a sample is linearly proportional to L^2/D . Then Eq. (2) is used to calculate the real thermal diffusivity of the sample. Detailed physical principle and equation deduction can be found in the Supporting information.

3. Results and discussion

3.1. Measurement of thermal diffusivity using the TET technique

Take sample 1–1 as an example, the fitting result is shown in Fig. 2b. Its measured thermal diffusivity is $2.64 \times 10^{-6} \text{ m}^2 \text{ s}^{-1}$. TET experiments are repeated on the same GF sample at three different lengths. Fig. 3 shows the linear fit of effective thermal diffusivity against L^2/D for sample 1. By linear fitting of data points and extending the fitting line to the y axis, we obtain an intersection point with the value of $2.08 \times 10^{-6} \text{ m}^2 \text{ s}^{-1}$, which is the real thermal diffusivity for the GF. The detailed parameters are listed in Table 1.

The volumetric specific heat of the sample is calculated from the calibration procedure and the steady state TET temperature rise. The calibration result of one GF sample is displayed in Fig. 2b (inset). The thermal conductivity is derived based on the expression $k = I^2 R L / (12 A \Delta T)$ as $1.19 \text{ W m}^{-1} \text{ K}^{-1}$. By using $\alpha = k / \rho c_p$, we can obtain volumetric specific heat $5.69 \times 10^5 \text{ J m}^{-3} \text{ K}^{-1}$.

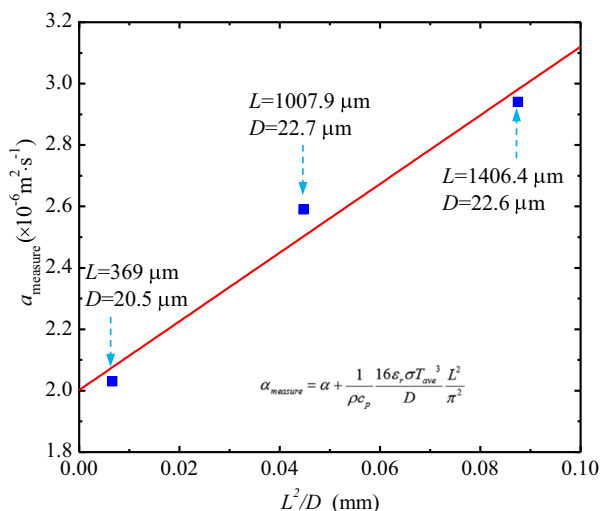


Fig. 3. Linear fitting of the effective thermal diffusivity change against L^2/D for GF sample 2. Symbols are the experimental results, and solid lines for linear fitting.

3.2. Physics behind the strong thermal conductivity reduction

The real thermal diffusivities of sample 1 and 2 are $2.08 \times 10^{-6} \text{ m}^2 \text{ s}^{-1}$ and $2.0 \times 10^{-6} \text{ m}^2 \text{ s}^{-1}$. And the conductivities are 1.14–1.18 W/m K. There is significantly reduced thermal transport in this GF when compared with single-layered graphene. It is really interesting to investigate the mechanisms behind this reduction in GF. First of all, from EDS and Raman results, we can get the conclusion that our continuous GF sample mainly consists of free-standing GO. The thermal conductivity of GO is much smaller than that of single layer graphene. The oxidized chemical structure introduced lattice defects which will greatly hinder thermal transport [16]. It has been illustrated that when graphite is oxidized, about 17% of the carbon atoms in the sample were oxygenated. The oxygen atom on the surface or edge of GO will reduce the phonon mean free path greatly [16]. So from the thermal conductivity equation $k = Cvl/3$, where C , v and l are the specific heat, the phonon wave velocity and the mean free path, the thermal conductivity will significantly decrease.

Second, as shown in Fig. 1c, some foldings and corrugations are clearly observed on the surface of the graphene/GO sheet. Phonons cannot pass through the wrinkled surface and will scatter on it. So the thermal conductivity reduction is partly ascribed to this wrinkled surface structure. Most importantly, strong phonon scattering will occur on the interface of adjacent graphene/GO flakes. The interlayer interactions and vibrational restrictions from neighboring layers limit the free vibration of the graphene/GO sheets and impose resistance on phonon transport [17]. The tangled nature of the graphene sheets in the fiber and lattice defects that are introduced during GO sheet synthesis and subsequent reduction processes can be another reason causing the extremely low thermal conductivity.

Last but not least, inspired from reference [18], the thermal contact resistance at the interface between the graphene/GO sheets is pretty large. This thermal contact resistance is considered to be two types: one occurs in the radial direction and the other one along the axis of the fiber. The second one is recognized as the main reason of the reduction in the overall thermal conductivity. The size of graphene/GO sheet is in the range of less than $3 \mu\text{m}$ [19], so there are many graphene/GO sheets stacked together along the axial direction of GF sample. The influence of the overall thermal contact resistance in the thermal transport should not be ignored. We speculate the main reason for ultralow thermal conductivity is the overall thermal contact resistance, rather than the phonon scattering.

4. Conclusions

In summary, thermal properties of GFs have been studied in this work. The thermal diffusivity of the suspended GF sample was measured at $(2.0\text{--}2.08) \times 10^{-6} \text{ m}^2 \text{ s}^{-1}$. From the calibration result, the volumetric specific heat was $5.69 \times 10^5 \text{ J m}^{-3} \text{ K}^{-1}$. The corresponding intrinsic thermal conductivity was 1.14–1.18 W/m K. This ultralow thermal conductivity is mainly attributed to the large thermal contact resistance between individual fibers and strong phonon scattering at boundaries. The result will benefit thermal design of GF-based thermal energy applications.

Acknowledgments

Support of this work from the National Natural Science Foundation of China (Nos. 51506106 and 11402180) are gratefully acknowledged.

Table 1
Details of GF samples characterized by using the TET technique.

Sample	L (μm)	D (μm)	R_{ave} (ohm)	Current (mA)	$\alpha_{\text{measure}} (\times 10^{-6} \text{ m}^2 \text{ s}^{-1})$	$\alpha_{\text{real}} (\times 10^{-6} \text{ m}^2 \text{ s}^{-1})$	$k_{\text{real}} (\text{W m}^{-1} \text{ K}^{-1})$
1-1	1410.4	22.3	6395.8	0.06	3.32	2.08	1.18
1-2	1035.4	26.2	6084.7	0.06	2.64		
1-3	437	20.3	2409.5	0.17	2.22		
2-1	1406.4	22.6	9326.3	0.038	2.94	2.00	1.14
2-2	1007.9	22.7	6381.4	0.05	2.59		
2-3	368.5	20.5	2590.1	0.13	2.03		

Appendix A. Supporting information

Supplementary data associated with this article can be found in the online version at <http://dx.doi.org/10.1016/j.matlet.2016.07.092>.

References

- [1] A.K. Geim, K.S. Novoselov, Nat. Mater. 6 (2007) 183–191.
- [2] Y.B. Zhang, Y.W. Tan, H.L. Stormer, et al., Nature 438 (2005) 201–204.
- [3] C. Lee, X.D. Wei, J.W. Kysar, et al., Science 321 (2008) 385–388.
- [4] A.A. Balandin, Nat. Mater. 10 (2011) 569–581.
- [5] A.A. Balandin, S. Ghosh, W.Z. Bao, et al., Nano Lett. 8 (2008) 902–907.
- [6] J.D. Renteria, S. Ramirez, H. Malekpour, et al., Adv. Funct. Mater. 25 (2015) 4664–4672.
- [7] J.D. Renteria, D.L. Nika, A.A. Balandin, Appl. Sci. 4 (2014) 525–547.
- [8] H. Malekpour, K.-H. Chang, J.-C. Chen, et al., Nano Lett. 14 (2014) 5155–5161.
- [9] H. Cheng, C. Hu, Y. Zhao, et al., NPG Asia Mater. 6 (2014) e113.
- [10] Z. Xu, C. Gao, Nat. Commun. 2 (2011) 1145–1154.
- [11] R. Jalili, S.H. Aboutalebi, D. Esrafilzadeh, et al., Adv. Funct. Mater. 23 (2013) 5345–5354.
- [12] M. Tian, L. Qu, X. Zhang, et al., Carbohydr. Polym. 111 (2014) 456–462.
- [13] Z. Xu, C. Gao, Nat. Commun. 2 (2011) 571.
- [14] J.Q. Guo, X.W. Wang, T. Wang, J. Appl. Phys. 101 (2007) 063537.
- [15] H. Lin, S. Xu, X. Wang, et al., Nanotechnology 24 (2013) 415706.
- [16] W. Yu, G. Liu, J. Wang et al. Synthesis and Reactivity in Inorganic, Metal-Organic, and Nano-Metal Chemistry, 43, 2013, pp. 1197–1205.
- [17] Z. Wei, Z. Ni, K. Bi, et al., Carbon 49 (2011) 2653–2658.
- [18] Y. Xie, S. Xu, Z. Xu, et al., Carbon 98 (2016) 381–390.
- [19] W. Yu, H. Xie, W. Chen, J. Appl. Phys. 107 (2010) 094317.